IONIC RELATIONS AND ULTRASTRUCTURE IN *ULVA LACTUCA*

By K. R. West* and M. G. Pitman*†

[*Manuscript received February* 13, 1967]

Summary

Measurements have been made of fluxes of potassium and sodium in *U. lactuca*. As far as potassium exchange is concerned, the non-free space acts as a single component; the rate of exchange of the 350 μ-equiv/g of potassium is apparently limited by the plasmalemma where the flux is about 100 μ-equiv/g fresh wt./hr. In the dark the flux drops by about 50%, and can be further reduced by inhibitors of oxidative phosphorylation.

Sodium exchange is characterized by two components in the non-free space; it is suggested that the flux at the plasmalemma is about 100 μ-equiv/g fresh wt./hr and that the flux at the tonoplast is only 1–3 μ-equiv/g fresh wt./hr.

A study of the structure of cells by electron microscopy showed the distribution of cytoplasm and chloroplast in these cells. A feature of particular interest was the well-developed golgi complex close to the nucleus.

I. Introduction

The common sea lettuce, *Ulva lactuca*,‡ like many other marine algae, contains very high levels of potassium relative to sodium. The tissue contains about 350 μ-equiv/g of potassium and 50 μ-equiv/g of sodium, while sea-water contains 10 and 500 μ-equiv/ml respectively of these ions. Scott and Hayward (1953*a*, 1953*b*, 1953*c*) showed that this selectivity was maintained by metabolically linked processes; an active potassium uptake and an active sodium excretion.

Similar explanations have been suggested to account for potassium selectivity in a number of other algae — *Nitellopsis obtusa* (MacRobbie and Dainty 1958), *Chara australis* (Hope and Walker 1960; Hope 1963), *Nitella translucens* (MacRobbie 1962), *Chaetomorpha darwinii* (Dodd, Pitman, and West 1966). In these examples it was possible to measure tracer fluxes at the plasmalemma and at the tonoplast. The active uptake of potassium and excretion of sodium appears to take place at the plasmalemma, and the fluxes may be coupled as in animal systems.

The purpose of this paper is to measure the fluxes of potassium and sodium in *Ulva*, in order to relate Scott and Hayward's work with inhibitors to the tracer and potential measurements made in other algae (as above). In addition a parallel study was made of the structure of the cells in order to try to locate the transport processes. The present paper therefore includes the results of a study of the structure using the electron microscope.

* Botany Department, University of Adelaide.

† Present address: School of Biological Sciences, University of Sydney.

‡ This species agrees in general morphology with the description of the European species *Ulva lactuca* given by Föyn (1955).

II. Materials and Methods

(a) *Uptake and Measurements*

Actively growing *U. lactuca* plants were collected from the piles of a jetty at Grange, South Australia. The plants were brought to the laboratory and kept at 17°C in aerated sea-water. Tissue kept in this way maintained the high K/Na ratio for a number of weeks. However, in no experiment were plants kept longer than 6 days before use.

Growth of the frond is diffuse, with cells in any part of the frond being capable of division. The fronds used in these experiments were approximately the same size (*c.* 12 sq. in.) and were near the maximum size for the species in this locality.

Samples 2–3 in. square were cut from fronds and placed in a glass tank illuminated by six fluorescent tubes (light treatments — light intensity 350 lumens/sq ft) or in large beakers covered with aluminium foil (dark treatment). All experiments were carried out at 17°C. Sodium and potassium were extracted by boiling three times in 1 in 10 nitric acid (total volume 15 ml) and determined by flame-photometry.

Radioactive tracer solutions were prepared by adding stock tracer to sea-water, and compensating for any change in the concentration of potassium. ^{24}Na and ^{42}K were obtained as irradiated carbonates from the Australian Atomic Energy Establishment, Lucas Heights, N.S.W., and converted to chlorides by titration with HCl.

(b) *Preparation of Material for Electron Microscopy*

Small pieces (1 by 0·5 mm) of *U. lactuca* were fixed for 35 min in either a 1·5% veronal acetate–potassium permanganate solution or a 2% unbuffered potassium permanganate solution. The fixative was initially cold. The pieces of tissue were rinsed, dehydrated in either a graded ethanol or acetone series, and embedded in Araldite. The Araldite was polymerized at 60°C for 2 days. Sections were cut with a Si-ro-flex ultramicrotome using glass knives and mounted on 200-mesh specimen grids coated with a carbon-stabilized Parlodion–amyl acetate film. Some sections were post-stained with lead citrate (Reynolds 1963).

Sections were observed using a Siemens Elmiskop 1A electron microscope operating at 60 kV with a variety of apertures.

III. Results

(a) *Potassium Tracer Exchange*

Fronds of *U. lactuca* grown in the light contain about 300–360 μ-equiv/g fresh weight of potassium; when kept in the dark for about 4 days this level falls to 260–280 μ-equiv/g fresh weight and stays steady at this level (see Scott and Hayward 1953*a*). When fronds are put into sea-water labelled with ^{42}K there is a rapid uptake of tracer and within 10 hr the specific activity of potassium is the same within the tissue as in the sea-water.

If tissue labelled in this way is transferred to unlabelled solutions there is again a rapid exchange as tracer diffuses out of the tissue. Figure 1 shows the amount of tracer in the tissue, and the rate of loss, plotted logarithmically, against time. The graph is linear and exchange of all the potassium behaved as a simple exponential

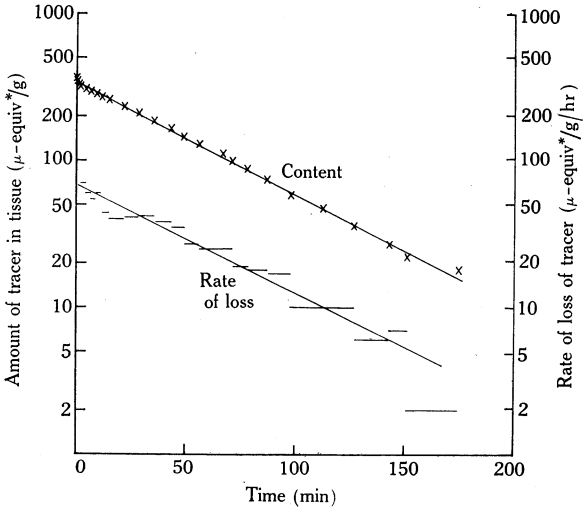

Fig. 1.—Loss of ^{42}K from *U. lactuca*. Amount of tracer in the tissue (content) and rate of loss are plotted logarithmically against time.

function, as if the potassium were all in one phase. In this case the exchange flux can be related to the exponential constant and the content of the tissue:

$$-(dQ^*/dt) = \phi_K(Q^*/Q), \tag{1}$$

where Q = amount of potassium in the tissue, Q^* = amount of tracer in the tissue, and ϕ_K = exchange flux of potassium. If $Q^* = Q_0^*$ at $t = 0$, then

$$Q^* = Q_0^* e^{-kt}, \tag{2}$$

where $k = \phi_K/Q$. It can also be shown that during uptake of isotope the amount of isotope increases as

$$Q^* = Q_{max}^*(1-e^{-kt}). \tag{3}$$

Q_{max}^* is equal to the amount of tracer in the tissue at isotopic equilibrium, i.e. *the specific activity of the labelling solution* (S_0) $\times$ *the amount of potassium in the tissue*, or $S_0 \times Q$.

Figure 2 shows a graph of $\log_e[(Q_{max}^* - Q^*)/Q_{max}^*]$ against time which is linear, as predicted by this model, but is a less accurate measure of k than may be obtained from Figure 1.

Estimates of flux of potassium made in this way are summarized in Table 1. Values of ϕ_K are means of duplicates in the isotope-loss experiments. The differences

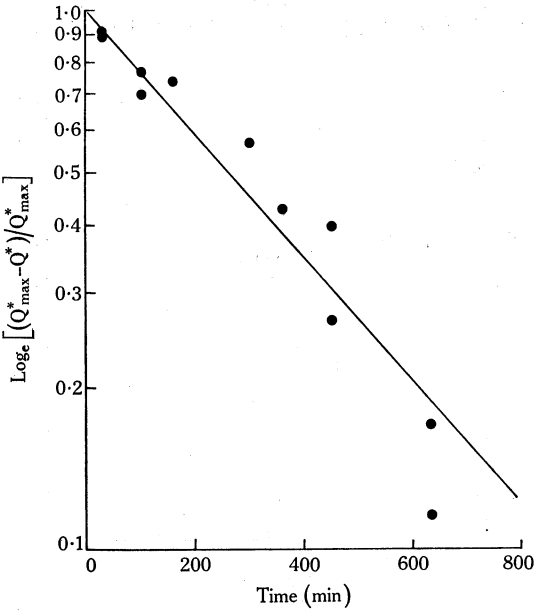

Fig. 2.—Uptake of ^{42}K by *U. lactuca*. The amount of isotope present at any time (Q^*) as a fraction of the amount of isotope present at flux equilibrium (Q^*_{max}) is plotted logarithmically against time.

between uptake 1, loss 1, and loss 2 experiments are due to differences in activity of the tissue, as differences between samples in the same experiment were only about 10%.

TABLE 1

EXCHANGE OF POTASSIUM BETWEEN *U. LACTUCA* AND SEA-WATER

Estimated error in $Q \pm 3\%$; in $\phi_K \pm 10\%$

Experiment	Condition	k (hr^{-1})	Q (μ-equiv/g)	ϕ_K (μ-equiv/g/hr)
Uptake 1	Light	0·30	305	90
	Dark	0·16	260	40
Loss 1	Light	0·21	335	70
	Dark	0·10	280	28
Loss 2	Light	0·35	365	130

The results show clearly that there is a reduction in potassium flux in the dark by nearly 50%. This reduction was presumably responsible for the drop in potassium content from 330 to 280 μ-equiv/g.

The surface area of 1 g of tissue is about 350 cm^2/g (i.e. the area of the flat surface of the tissue). The surface area of the cells is very much larger (about 2000–3000 cm^2/g). The interpretation of an uptake of 100 μ-equiv/g/hr in relation to cell area depends on whether it is taking place over the whole of the cell surface or only that part directly exposed to the sea-water. Although the surfaces of the cell within the frond have only a short diffusion path between them and the sea-water, the cytoplasm is extremely thin in the inner parts of the cell, and most of the active transport may be restricted to the outer part of the cell where there is a large bulk of cytoplasm (see Plate 1, Figs. 1 and 2).

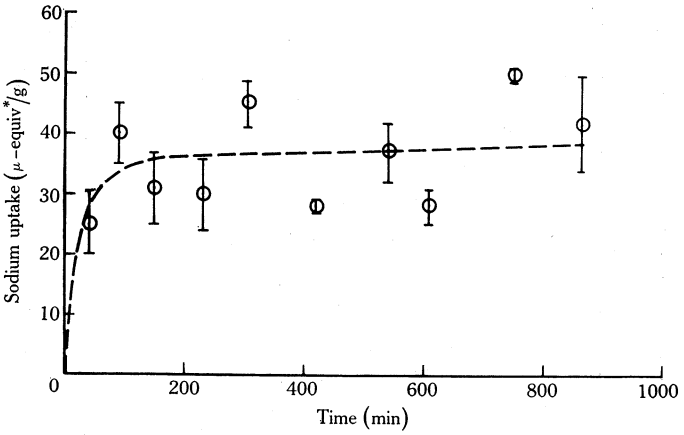

Fig. 3.—Uptake of ^{24}Na by *U. lactuca* plotted against time. Free-space sodium was removed by washing for 30 sec in 0·5M $CaCl_2$. Each point represents the mean of four samples. Highest and lowest point of each mean is also plotted (horizontal bars).

(*b*) *Exchange of Tracer Sodium*

Tissue which was blotted to remove surface sea-water contained about 500 μ-equiv/g of sodium, but if the tissue was rinsed in 0·5M $CaCl_2$ for 30 sec the sodium content was reduced to about 40–50 μ-equiv/g. Further rinses with $CaCl_2$ produced little further reduction. A similar loss of about 450 μ-equiv/g occurred both at 0·5°C and at 17°C, so it appears that this represents sodium in the free space.

This large free-space component must be washed out before tracer uptake can be measured to the non-free space. This method is not particularly accurate and there is a big scatter in the determinations. Figure 3 shows the time course of uptake measured in this way; despite the variability it is clear that there is an initial rapid uptake of about 30 μ-equiv/g. The specific activity of this non-free-space sodium was only about 80%; hence it appears that there is a part of this sodium that does not exchange rapidly.

This suggestion that there are two parts to the non-free-space exchange is confirmed by measurements of the rate of loss of isotope from the tissue to unlabelled sea-water (Fig. 4). This graph can be analysed into two exponential components,

one with a very short time for half-exchange (about 10 min) and the other with a longer time for half-exchange (200 min).

It appears as if there are two regions in the tissue. For each of these regions it is possible to estimate a content (Q_1, Q_2) and a flux (ϕ_1, ϕ_2). As ϕ_1 is very much larger than ϕ_2, the following simplified calculation can be used, which ignores the spatial

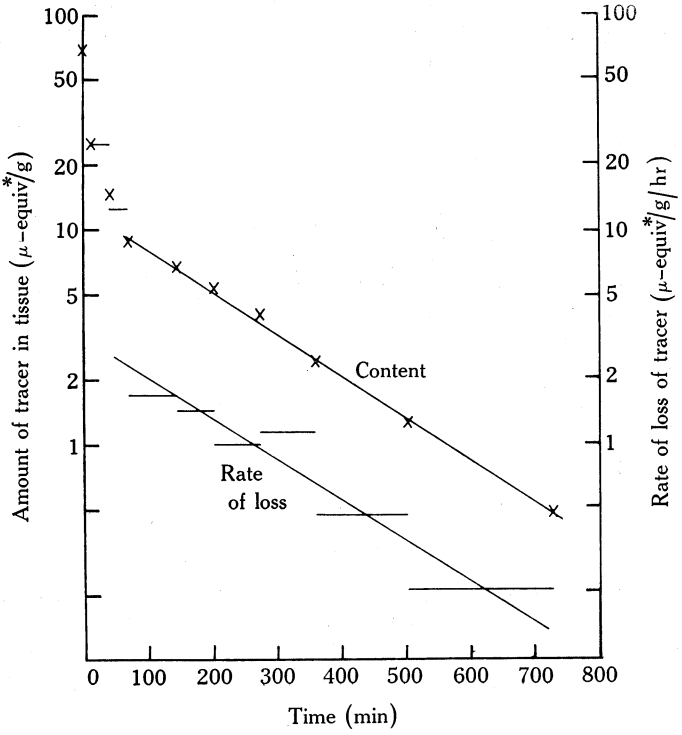

Fig. 4.—Loss of ^{24}Na from *U. lactuca*. Amount of tracer in the tissue (content) and rate of loss are plotted logarithmically against time.

relationship of the two regions. Firstly the total amount of isotope in the tissue is the sum of two exponential components, i.e.

$$\text{Amount of isotope} = (Q_1^*)_0 \, e^{-k_1 t} + (Q_2^*)_0 \, e^{-k_2 t}.$$

(This is equivalent to the upper line of Fig. 4). The rate of loss from the phases is the differential of the above expression, i.e.

$$\text{Rate of loss} = -k_1(Q_1^*)_0 \, e^{-k_1 t} - k_2(Q_2^*)_0 \, e^{-k_2 t}.$$

As the more rapid component becomes depleted both amount and rate of loss, when plotted as in Figure 4, tend to straight lines of the same slope. From data such as are shown in this figure, values of $(Q_1^*)_0$, k_1, $(Q_2^*)_0$, and k_2 can be estimated.

At the start of the exchange the specific activity in phase 1 was effectively that of the labelling solution (S_0), as exchange in this phase was very rapid. Hence

$(Q_1^*)_0$ divided by S_0 is equal to Q_1, the amount of sodium in phase 1. As $k_1 = \phi_1/Q_1$ (as for potassium), ϕ_1 can then be estimated. Results of two experiments are shown in Table 2. Each set is the mean of duplicate samples. At $t = 0$, the rate of loss of

TABLE 2

SODIUM FLUX (ϕ_1) AND CONTENT (Q_1) OF PHASE 1 (RAPID PHASE)

Experiment	Condition	k_1 (hr^{-1})	Q_1 (μ-equiv/g)	ϕ_1 (μ-equiv/g/hr)
Loss 1	Light	$3{\cdot}1 \pm 0{\cdot}1$	28 ± 4	85 ± 15
Loss 2	Light	$4{\cdot}2 \pm 0{\cdot}4$	27 ± 1	110 ± 10

tracer from the slow phase (phase 2) is equal to the flux (ϕ_2) times the specific activity of sodium in that phase (S_2). S_2 can be calculated from k_2, for during uptake (cf. potassium uptake)

$$S_2 = S_0(1 - e^{-k_2 t}),$$

and then Q_2 can be estimated either from $Q_2 = \phi_2/k_2$ or $Q_2 = Q_2^*/S_2$. Values of k_2, Q_2, and ϕ_2 are given in Table 3.

TABLE 3

VALUES OF k_2, Q_2, AND ϕ_2 FOR SODIUM IN PHASE 2 (SLOW PHASE)

Experiment	Condition	k_2 (hr^{-1})	Q_2 (μ-equiv/g)	ϕ_2 (μ-equiv/g/hr)
Loss 1	Light	$0{\cdot}26 \pm 0{\cdot}01$	12 ± 2	$3{\cdot}1 \pm 0{\cdot}7$
Loss 2	Light	$0{\cdot}053 \pm 0{\cdot}003$	14 ± 1	$0{\cdot}7 \pm 0{\cdot}1$

The two experiments in these tables were carried out with different collections of tissue, which could account for the difference in ϕ_2. Apart from this difference,

TABLE 4

COMPARISON OF ^{42}K AND ^{86}Rb UPTAKE

	^{42}K	^{86}Rb
Tracer uptake in 26 hr (μ-equiv/g)	320	43
Specific activity of tissue	1·0	0·13
ϕ_1 (μ-equiv/g/hr)	44	24
ϕ_2 (μ-equiv/g/hr)	Very large	1·4

there is reasonable agreement between estimates of Q_1 and Q_2, giving a total non-free space estimate of about 40 μ-equiv/g, which is consistent with the measurements of total and free-space sodium (Fig. 3).

(c) *Rubidium Tracer Exchange*

^{86}Rb does not act as a tracer for potassium in cells of *U. lactuca* (West and Pitman 1967). Uptake of potassium is rapid and the whole of the potassium in the cells soon comes to flux equilibrium. Uptake of rubidium is initially rapid (about 40 μ-equiv/g/hr) but then slows down to about 2 μ-equiv/g/hr.

Rubidium uptake, like sodium uptake, is definitely biphasic in contrast to the apparent single phase of potassium uptake. Table 4 compares fluxes of potassium and rubidium. The values for potassium fluxes are lower than those previously quoted, but were made at a different time of the year.

IV. Structure

(a) *General*

Studies of members of the Chlorophyta using the electron microscope include those by Sager and Palade (1957), Friedman and Manton (1960), Moner and Chapman (1960), Hoffman and Manton (1963), Lang (1963), Trezzi, Galli, and Bellini (1964), Manton (1964), and Deason (1965). Some characean species have also been described (Crawley 1964; Chambers and Mercer 1964). There are few published accounts of a detailed electron-microscope study of a multicellular green alga, thus the cells of *U. lactuca* will be described in some detail.

The vegetative cells of *U. lactuca* consist of cell wall, single chloroplast (which may occupy a considerable volume of the cell), cytoplasm, and vacuole (Plate 1, Fig. 2). The general appearance of vegetative cells is shown in Plates 1 and 2. Plasmolysis of the cells occurred often, but was reduced when unbuffered permanganate was used as a fixative.

(b) *Subcellular Organization*

(i) *The Chloroplast.*—The chloroplast of *U. lactuca* is described as a single chloroplast by light microscopists (Föyn 1955). When observed with the electron microscope the chloroplast often appears in several places in the cell (Plate 1, Fig. 2) probably indicating that the outer boundary of the chloroplast is convolute. The photosynthetic chloroplast lamellae are very densely packed and in some micrographs (cf. Plate 1, Fig. 2) appear to form flat disks similar to other algal chloroplasts described by Gibbs (1962). Pyrenoids (1–3) similar to those described by Gibbs (1962) for *Chaetomorpha* are commonly found in the chloroplast and consist of a starch sheath surrounding a pyrenoid matrix, which is traversed by two membranes (Plate 4, Fig. 1). Favourable sections show the space between the two membranes to be an extensive vacuole (Plate 4, Figs. 2, 3, and 4). Small vesicles about 0·1 μ in diameter appear to be forming in the chloroplast stroma and merging with the vacuole (Plate 4, Figs. 3 and 4), suggesting a form of reverse "pinocytosis" at the ultrastructural level. Starch grains other than those associated with the pyrenoid occur throughout the chloroplast and distort the chloroplast lamellae. The grains appear to be enclosed by slightly modified lamellae.

(ii) *The Nucleus.*—The nucleus of the cell of *U. lactuca* is regular in appearance, circular to ovoid (*c.* 3 μ in diameter) with a small but pronounced flattened region

(Plate 1, Fig. 2; Plate 2, Fig. 2). The nuclear membrane is double, contains pores (Plate 1, Fig. 2), and may well be continuous with the endoplasmic reticulum of the cytoplasm (Plate 1, Fig. 2; Plate 2, Fig. 2).

(iii) *Golgi Complex and Endoplasmic Reticulum.*—The cytoplasm of *U. lactuca* contains a number of golgi bodies located near the nucleus (Plate 1, Fig. 2; Plates 2 and 3). These golgi bodies are arranged in a ring near the flattened side of the nucleus and are surrounded by endoplasmic reticulum (Plate 2, Fig. 2). There are 6–8 cisternae in each golgi with the cisternae on the inner face being more swollen than those nearest the endoplasmic reticulum. Each golgi appears to be forming a large number of golgi vesicles which collect in the centre of the ring. Most of these vesicles are electron-translucent, although there are a few darkly staining membrane-bound vesicles (Plate 3, Fig. 2). The appearance of each golgi body in those sections parallel to the thallus surface (Plate 3, Figs. 1 and 2; Plate 2, Fig. 2) is rather different to that normally seen in plant cells although the sections perpendicular to the surface (Plate 3, Figs. 3 and 4) show the more usual structure.

(iv) *Mitochondria.*—Mitochondria are numerous and are usually about 0·5 μ in length and slightly narrower than long. Cristae arise irregularly as infoldings of the inner membrane, but do not appear to be as numerous as the cristae of higher plant mitochondria. Mitochondria are concentrated in the region of the golgi complex, but are not enclosed by the ring of golgi bodies (Plate 3, Fig. 1).

V. Discussion

The results of the tracer studies of exchange in the non-free space may be summarized as follows:

(1) There is a very rapid exchange of the 300–360 μ-equiv/g of potassium, equivalent to a flux of about 100 μ-equiv/g/hr. The exchange appears to be from one region.

(2) Sodium exchange appears to take place from two regions. One containing about 28 μ-equiv/g with an exchange flux of 85–110 μ-equiv/g/hr. The other contains about 12 μ-equiv/g and has a much slower exchange of about 1–3 μ-equiv/g/hr, though there was some variability in this flux between different collections of tissue.

The flux of potassium measured in these experiments clearly involves all the 300–360 μ-equiv/g in the tissue. In order to maintain suitable internal osmotic pressures, much of this potassium must be in the vacuole; it cannot be in the cytoplasm alone. Measurements of total tracer uptake are only 10 μ-equiv/g larger than the tracer taken up to the non-free space, and the total tracer uptake is equal to that determined chemically. There does not appear to be any part that is not accounted for, so the non-free space potassium can therefore be reasonably assumed to be distributed between both cytoplasm and vacuole, and the limiting flux is that across the plasmalemma.

The distribution of sodium in two phases is analogous to that described for many other algal cells, where the two phases have been shown to be due to cytoplasm and vacuole. If this model is assumed to apply to *U. lactuca* as well, then a possible interpretation of the results is as set out in Table 5.

However, there are complications in applying this model to *U. lactuca* cells. The chloroplast is commonly in a cap at one end of the cell in at least 50% of the cytoplasm. The rest of the cytoplasm contains mitochondria and golgi bodies. All these organelles are potential sites for ion accumulation and so make it impossible to estimate the concentration in the cytoplasm.

Another problem is the estimation of the size of the fluxes (relative to surface areas). It seems improbable that there could be a clearly marked biphasic uptake of sodium in the very thin regions of the cytoplasm away from the chloroplast, as plasmalemma and tonoplast are almost touching here (Plate 1, Fig. 2). In addition

TABLE 5

POTASSIUM AND SODIUM FLUXES IN *U. LACTUCA*

Units of flux are μ-equivalents/g/hr

	Outer boundary (plasmalemma)		Inner boundary (tonoplast)
Sea-water Potassium 10μ-equiv/ml Sodium 500 μ-equiv/ml		Potassium content 300–360 μ-equiv/g	Potassium content 300–360 μ-equiv/g
	100	Potassium flux	Very large
		Sodium content 28 μ-equiv/g	Sodium content 14 μ-equiv/g
	85–110	Sodium flux	1—3

the active transport may well be localized in a region of the cell near the chloroplast and in only one end of the cell. "Flux equilibrium" in these cells may not be the same as in the giant algal cells where an active transport is balanced by passive fluxes of the same magnitude over the same area of the cell. In *U. lactuca* there could well be an active flux *in one part of the cell* balanced by a passive flux over the *whole* cell. For example, the surface area of the cell is about 3000 cm^2/g of tissue and the potassium influx of 100 μ-equiv/g/hr over this area is equivalent to 10 pmoles/cm^2/sec. If the active flux is confined to the region of dense cytoplasm (about one-quarter of the cell surface) flux equilibrium could be brought about by an active flux of 40 pmoles/cm^2/sec over one-quarter of the cell surface balanced by an efflux of 10 pmoles/cm^2/sec over the whole cell.

These problems of interpretation do not invalidate some of the observations. At the plasmalemma the potassium influx appears to be active, as it was reduced in the dark and could be further reduced in the dark by respiratory uncouplers (carbonyl cyanide *m*-chlorophenyl hydrazone or dinitrophenol), leading to a large net

loss of potassium from the cell. Due to the small size of the cells no really satisfactory measurements were made of transcellular potentials but the vacuole is at least 60 mV negative to the solution and there must therefore be an active sodium efflux. According to the model used above, the fluxes of potassium and sodium at the plasmalemma appear to be about the same size.

The fluxes of sodium and potassium at the inner boundary are certainly very different and show that net uptake of sodium to the cell would be limited by diffusion across the tonoplast. In measurements of changes of net flux, such as those made by Scott and Hayward (1953*a*) the net flux of sodium would have been limited by this boundary, but the net uptake of potassium would have been limited by the plasmalemma, as we have seen. Here, then, is a simple explanation for the differences they found in the kinetics of sodium and potassium exchange.

The measurements of rubidium uptake show that the main distinction between potassium and rubidium transport takes place within the cell, so presumably at the tonoplast. The difference between fluxes of potassium and rubidium at the plasmalemma is only about 50%, but at the tonoplast there is a reduction from about 500 μ-equiv/g/hr to about 2 μ-equiv/g/hr (the tonoplast flux of potassium must be about five times the plasmalemma flux to maintain a single phase exchange, i.e. about 500 μ-equiv/g/hr). This level of discrimination is remarkable and suggests that transport of potassium across the tonoplast is largely a special metabolic process.

A noteworthy feature of the cytoplasmic organization is the golgi complex which is always found close to the nucleus on the side away from the chloroplast (i.e. towards the vacuole). Suggestions as to the role of golgi bodies in the general metabolism of cells are many and varied. The golgi body has been considered important in the development of secondary wall formation in xylem vessels (Wooding and Northcote 1964), vacuole formation in developing shoot apices (Marinos 1963), while a very similar type of golgi body is thought to be involved in secretion of water droplets in the alga *Glaucocystis* (Schnepf and Koch 1966). A number of workers, using both animal (Sjöstrand and Hanson 1954) and plant material (Schnepf 1960, 1961; Mollenhauer, Whaley, and Leech 1961; Mollenhauer 1965) also consider that golgi bodies may be concerned with protein synthesis [see Mollenhauer and Morre (1966) for a review of the role of the golgi apparatus in plant cells].

The golgi complex in *U. lactuca* is certainly very active and large numbers of golgi vesicles are produced in each cell. It is tempting to assign to the complex a role in ion transport across the cytoplasm and more particularly to potassium secretion into the vacuole. If this is so then the very selective uptake of potassium over rubidium may be a direct result of the activity of the golgi complex.

In summary, *U. lactuca*, like other marine organisms, maintains high levels of potassium and low sodium content by active excretion of sodium and accumulation of potassium. Since in *U. lactuca* the cytoplasm constitutes a major part of the cell, this species is particularly useful for studying some aspects of active transport.

VI. Acknowledgment

One of us (K.R.W.) gratefully acknowledges the receipt of a Commonwealth Post-Graduate Award.

VII. References

Chambers, T. C., and Mercer, F. V. (1964).—Studies on the comparative physiology of *Chara australis*. II. The fine structure of the protoplast. *Aust. J. biol. Sci.* **17**, 372.

Crawley, J. C. W. (1964).—Cytoplasmic fine structure in *Acetabularia*. *Expl Cell Res.* **35**, 497.

Deason, T. R. (1965).—Some observations on the fine structure of vegetative and dividing cells of *Chlorococcum*. *J. Phycol.* **1**, 97.

Dodd, W. A., Pitman, M. G., and West, K. R. (1966).—Sodium and potassium transport in the marine alga *Chaetomorpha darwinii*. *Aust. J. biol. Sci.* **19**, 341.

Föyn, B. (1955).—Specific differences between northern and southern European populations of the green alga *Ulva lactuca* L. *Pubbl. Staz. zool. Napoli* **27**, 261.

Friedman, I., and Manton, I. (1960).—Gametes, fertilization and zygote development in *Prasiola stipitata*. *Nova Hedwigia* **1**, 333.

Gibbs, S. P. (1962).—The ultrastructure of the pyrenoids of the green algae. *J. Ultrastruct. Res.* **7**, 262.

Hoffman, L. R., and Manton, I. (1963).—Observations on the fine structure of *Oedogonium*. II. The spermatozoid of *O. cardiacum*. *Am. J. Bot.* **50**, 455.

Hope, A. B. (1963).—Ionic relations of cells of *Chara australis*. VI. Fluxes of potassium. *Aust. J. biol. Sci.* **16**, 429.

Hope, A. B., and Walker, N. A. (1960).—Ionic relations of cells of *Chara australis*. III. Vacuolar fluxes of sodium. *Aust. J. biol. Sci.* **13**, 277.

Lang, N. J. (1963).—Electron microscopy of the Volvocaceae and Astrephomenaceae. *Am. J. Bot.* **50**, 280.

MacRobbie, E. A. C. (1962).—Ionic relations of *Nitella translucens*. *J. Gen. Physiol.* **45**, 861.

MacRobbie, E. A. C. (1965).—The nature of the coupling between light energy and active ion transport in *Nitella translucens*. *Biochim. Biophys. Acta* **94**, 64.

MacRobbie, E. A. C., and Dainty, J. (1958).—Ion transport in *Nitellopsis obtusa*. *J. Gen. Physiol.* **42**, 335.

Manton, I. (1964).—Observations on the fine structure of the zoospore and young germling of *Stigeoclonium*. *J. exp. Bot.* **15**, 399.

Marinos, N. G. (1963).—Vacuolation in plant cells. *J. Ultrastruct. Res.* **9**, 177.

Mollenhauer, H. H. (1965).—Transition forms of Golgi apparatus secretion vesicles. *J. Ultrastruct. Res.* **12**, 439.

Mollenhauer, H. H., and Morre, D. J. (1966).—Golgi apparatus and plant secretion. *A. Rev. Pl. Physiol.* **17**, 27.

Mollenhauer, H. H., Whaley, W. G., and Leech, J. H. (1961).—A function of the Golgi apparatus in outer root cap cells. *J. Ultrastruct. Res.* **5**, 193.

Moner, J. D., and Chapman, G. B. (1960).—The development of the adult cell form in *Pediastrum biradiatum* as revealed by the electron microscope. *J. Ultrastruct. Res.* **4**, 26.

Reynolds, E. S. (1963).—The use of lead citrate at high pH as an electron-opaque stain in electron microscopy. *J. Cell Biol.* **17**, 208.

Sager, R., and Palade, G. E. (1957).—Structure and development of the chloroplast in *Chlamydomonas*. I. The normal green cell. *J. Biophys. Biochem. Cytol.* **3**, 463.

Schnepf, E. (1960).—Zur Feinstruktur der Drüsen von *Drosophyllum lusitanicum*. *Planta* **54**, 641.

Schnepf, E. (1961).—Licht- und elektronenmikroskopische beobachtungen an insektivorendrüsen über die secretion des fangschleimes. *Flora* **151**, 73–87.

Schnepf, E., and Koch, W. (1966).—Golgi apparatus and water secretion in *Glaucocystis*. *Z. Pflanzenphysiol.* **55**, 97.

Scott, G. T., and Hayward, H. R. (1953*a*).—Metabolic factors influencing the sodium and potassium distribution in *Ulva lactuca*. *J. Gen. Physiol.* **36**, 659.

Scott, G. T., and Hayward, H. R. (1953*b*).—The influence of iodacetate on the sodium and potassium content of *Ulva lactuca* and the prevention of its influence by light. *Science, N.Y.* **117**, 719.

Scott, G. T., and Hayward, H. R. (1953*c*).—The influence of temperature and illumination on the exchange of potassium ion in *Ulva lactuca*. *Biochim. Biophys. Acta* **12**, 401.

SCOTT, G. T., and HAYWARD, H. R. (1954).—Evidence for the presence of separate mechanisms regulating potassium and sodium distribution in *Ulva lactuca*. *J. Gen. Physiol.* **37**, 601.

SCOTT, G. T., and HAYWARD, H. R. (1955).—Sodium and potassium regulation in *Ulva lactuca* and *Valonia macrophysa*. In "Electrolytes in Biological Systems". (Ed. A. M. Shanes.) (Am. Physiol. Soc.: Washington.)

SCOTT, G. T., DE VOE, R., HAYWARD, H. R., and CRAVEN, G. (1957).—Exchange of sodium ion in *Ulva lactuca*. *Science, N.Y.* **125**, 160.

SJÖSTRAND, F. S., and HANZON, V. (1954).—Ultrastructure of Golgi apparatus of exocrine cells of mouse pancreas. *Expl Cell Res.* **7**, 415–20.

TREZZI, F., GALLI, M. G., and BELLINI, E. (1964).—L'infrastruttura di *Dunaliella salina*. *G. Bot. Ital.* **71**, 127.

WEST, K. R., and PITMAN, M. G. (1967).—Rubidium as a tracer for potassium in the marine algae *Ulva lactuca* and *Chaetomorpha darwinii*. *Nature, Lond.* **214**, 1262.

WOODING, F. B. P., and NORTHCOTE, D. H. (1964).—The development of the secondary wall of the xylem in *Acer pseudolatamus*. *J. Cell Biol.* **23**, 327.

EXPLANATION OF PLATES 1–4

PLATE 1

Fig. 1.—Light micrograph of a transverse section through the frond of *U. lactuca*. The frond is two cells thick with each cell being slightly longer than wide. The chloroplast and cytoplasm is concentrated in each cell near the thallus surface. The vacuole (*V*) occupies about 60% of the cell. The thick gelatinous cuticle (*C*) is clearly seen. ×730.

Fig. 2.—Low-power electron micrograph showing three cells each containing cytoplasm with a nucleus (*N*), chloroplast with pyrenoid (*P*), and golgi complex (*GC*). The chloroplast is usually single and localized in one part of the cell but in some cells it appears in part of the very thin cytoplasmic region (arrow). Chloroplast lamellae (*L*) occasionally appear to form grana-like structures. *V*, vacuole. *CW*, cell wall. ×12,600.

PLATE 2

Fig. 1.—Low-power electron micrograph of cells sectioned parallel to the thallus surface. The cells are plasmolysed, but the cell wall (*CW*), chloroplast (*Ch*), nuclei (*N*), and vacuoles (*V*) are clearly seen. A golgi complex (GC) is seen near each nucleus. The golgi are arranged in a circle 3–4 μ in diameter. Note the extremely thin layer of cytoplasm in some parts of the cell. ×5,400.

Fig. 2.—The Golgi complex at a higher magnification. There are eight Golgi bodies (*GB*), with swollen cisternae arranged in a circle adjacent to a flattened side of the nucleus (*N*). An enveloping layer of endoplasmic reticulum (*ER*), mitochondria (*M*), and the vacuole (*V*) are seen. ×27,500.

PLATE 3

Fig. 1.—Section cut parallel to the thallus surface showing the nucleus (*N*) and golgi complex (*GC*). The mitochondria (*M*) surround the ring of golgi bodies, but are not found in the centre of the ring where the golgi vesicles appear to collect. The mitochondria appear to have fewer cristae than higher plant mitochondria. Part of the chloroplast (*Ch*) with starch grains (*St*) is shown. *N*, nucleus. *V*, vacuole. ×17,100.

Fig. 2.—Detail of an area similar to that shown in Plate 3, Figure 1. Five golgi bodies (*GB*) are shown, each sectioned at a different level. One golgi body (arrow) is sectioned in such a way to show the cisternae and numerous golgi vesicles being formed. Small, darkly staining, membrane-bound vesicles (*Ve*) were often observed among the golgi vesicles. ×28,000.

Fig. 3.—Section cut transverse to the thallus surface showing nucleus (*N*), golgi bodies (*GB*), and golgi vesicles. The chloroplast (*Ch*) with starch grains (*St*) and clearly defined lamellae is also shown. ×19,800.

Fig. 4.—High-magnification micrograph showing a single golgi body. The large number of golgi vesicles (*Ve*) which each golgi body produces is clearly seen. The tonoplast membrane (*T*) and vacuole (*V*) are well defined. ×65,000.

Plate 4

Fig. 1.—Part of the chloroplast and cytoplasm of *U. lactuca* showing two pyrenoids (*P*) as they normally appear. Each pyrenoid consists of a starch sheath (*St*) surrounding a pyrenoid matrix which is divided by a double membrane (arrow). ×22,000.

Fig. 2.—Pyrenoid (*P*) sectioned in such a way as to show the space between the two membranes as a relatively large vacuole (*PV*). Mitochondria (*M*) and a nucleus (*N*) are shown in the cytoplasm. ×28,700.

Fig. 3.—Pyrenoid sectioned exactly in the plane of the two membranes revealing an extensive pyrenoidal vacuole (*PV*). Many small vesicles (0·1 μ in diameter) surround the vacuoles. ×25,000.

Fig. 4.—Chloroplast showing starch sheath (*St*) and pyrenoidal vacuole (*PV*). Three small vesicles (arrows) which appear to be discharging their contents into the pyrenoidal vacuole are shown. ×30,800.

IONIC RELATIONS AND ULTRASTRUCTURE IN *U. LACTUCA*

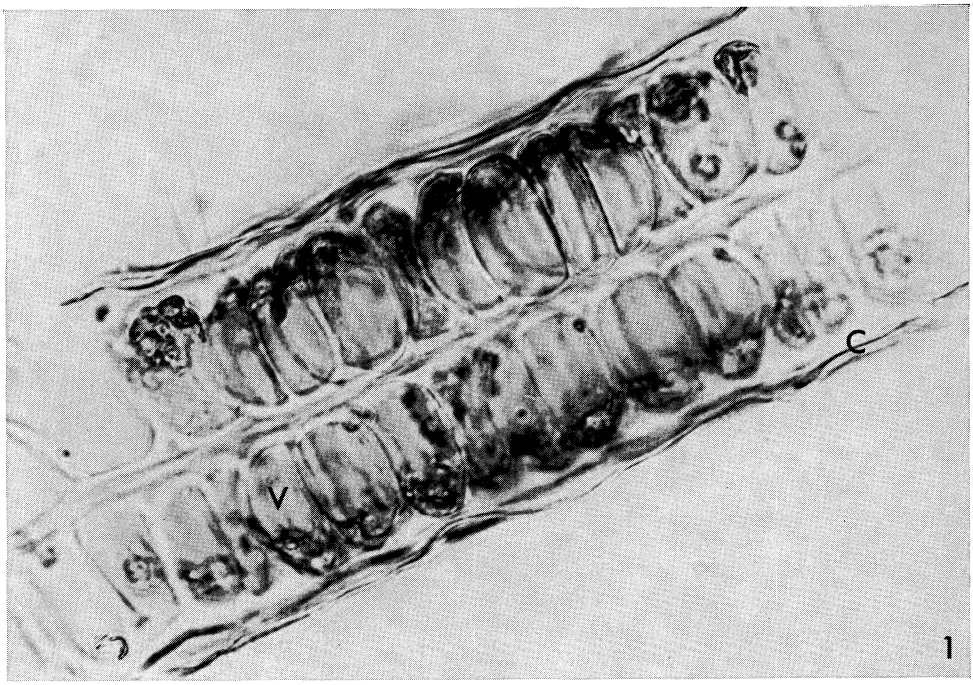

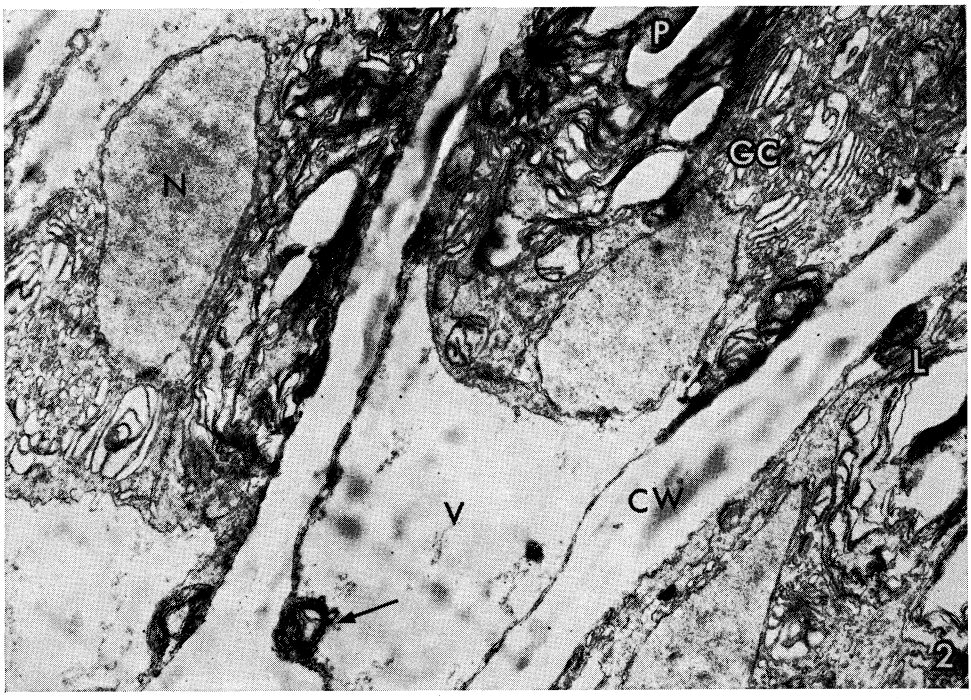

IONIC RELATIONS AND ULTRASTRUCTURE IN *U. LACTUCA*

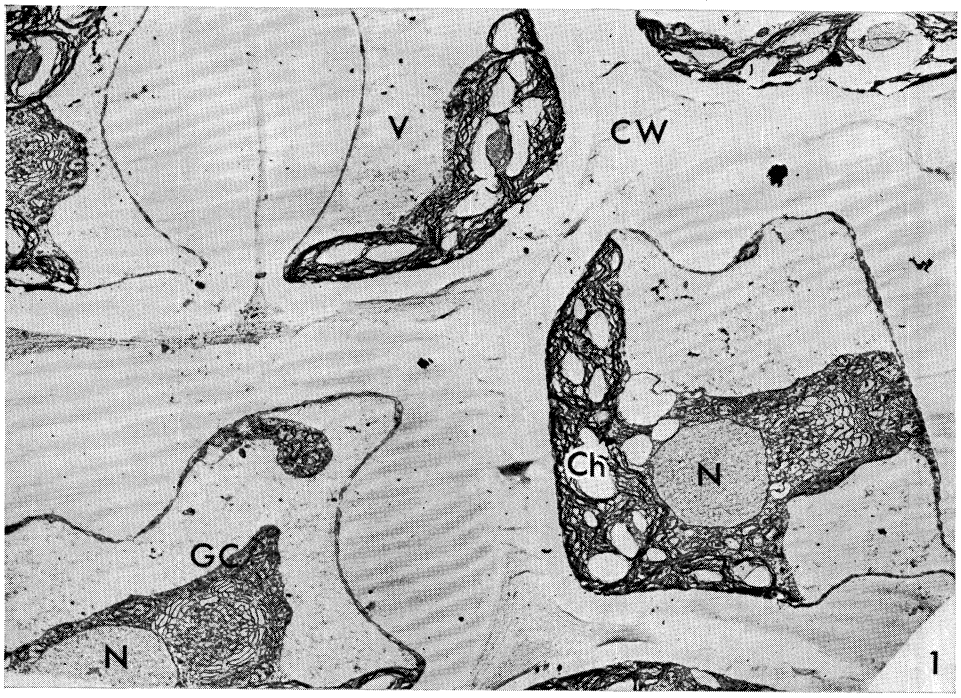

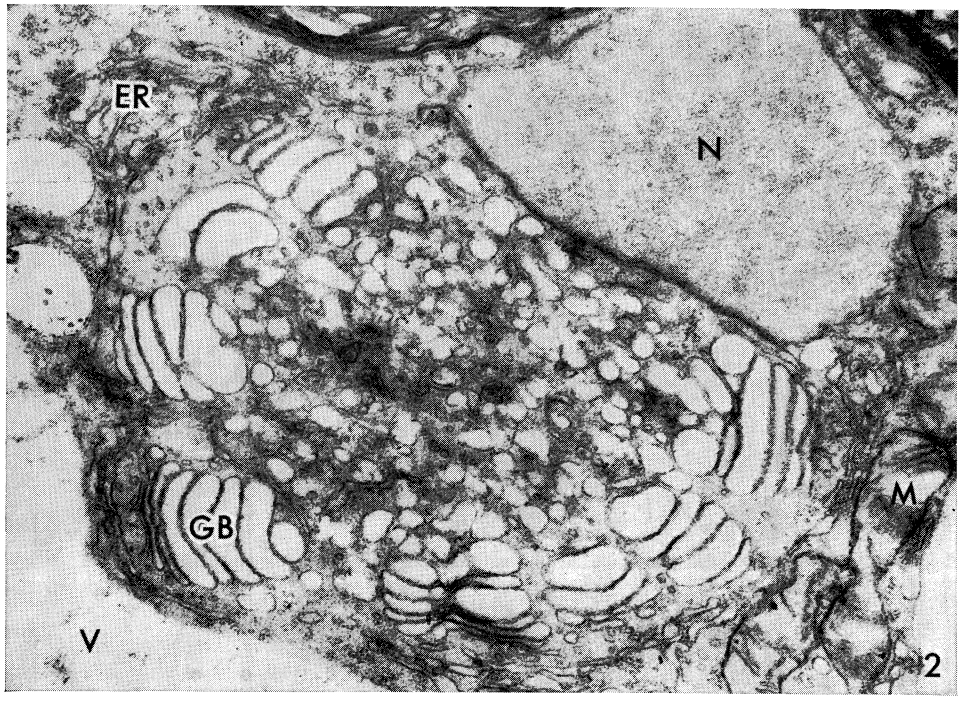

IONIC RELATIONS AND ULTRASTRUCTURE IN *U. LACTUCA*

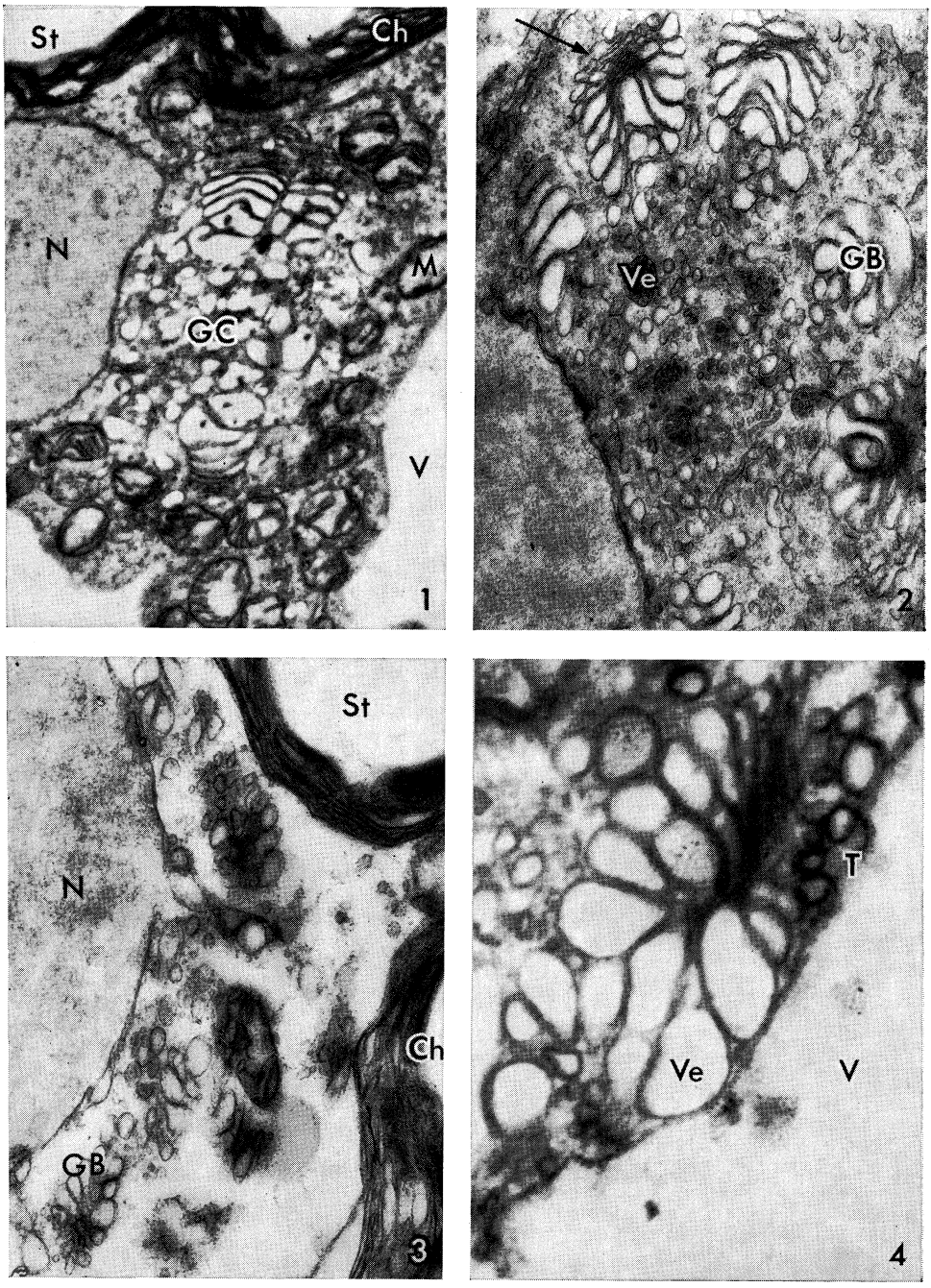

IONIC RELATIONS AND ULTRASTRUCTURE IN *U. LACTUCA*